High-pressure, transport, and thermodynamic properties of $CeTe_3$

D. A. Zocco, J. J. Hamlin, T. A. Sayles, and M. B. Maple
Department of Physics and Institute for Pure and Applied Physical Sciences, University of California–San Diego, La Jolla, California 92093, USA

J.-H. Chu and I. R. Fisher
Department of Applied Physics, Geballe Laboratory for Advanced Materials, Stanford University, Stanford, California 94305, USA
(Received 5 January 2009; revised manuscript received 19 March 2009; published 23 April 2009)

We have performed high-pressure, electrical resistivity, and specific heat measurements on $CeTe_3$ single crystals. Two magnetic phases with nonparallel magnetic easy axes were detected in electrical resistivity and specific heat at low temperatures. We also observed the emergence of an additional phase at high pressures and low temperatures and a possible structural phase transition detected at room temperature and at 45 kbar, which can possibly be related with the lowering of the charge-density wave transition temperature known for this compound.

DOI: 10.1103/PhysRevB.79.134428 PACS number(s): 62.50.−p, 71.27.+a, 75.25.+z, 71.45.Lr

I. INTRODUCTION

Charge- and spin-density waves (CDWs and SDWs) frequently occur in low-dimensional materials and are driven by electron-phonon and electron-electron interactions. These phases are formed by nesting of the Fermi surface, which can be perfect in one-dimensional systems.[1] A perfect nesting CDW system refers to the situation where all the electrons near the Fermi surface are excited with the same q vector of a particular phonon mode. On the other hand, incomplete nesting takes place for higher dimensional materials, for which a density wave gap opens only over certain regions of the Fermi surface. Rare-earth tritellurides RTe_3 (R=La-Tm, except for Eu) constitute a class of quasi-two-dimensional materials that has recently attracted a considerable amount of attention because the electronic properties of these materials can be changed by substituting one rare-earth element for another, making them ideal candidates for investigating the properties of the CDW state.[2–4] The rare-earth tritellurides crystallize in the $NdTe_3$ structure that belongs to the space group *Cmcm* (No. 63); the structure consists of alternating double layers of nominally square-planar Te sheets and corrugated double RTe layers and forms a weakly orthorhombic lattice.[5] In this standard space group denomination, the b axis is oriented perpendicular to the ac planes and the average lattice parameters for all the lanthanide series are (a, b, and c) $\sim(4,26,4)$ Å. It is evident that these compounds are electronically anisotropic, with the Te planes quite decoupled from the RTe slabs.[6,7] For this family of materials, the lattice modulation is characterized by a single inplane wave vector, which has approximately the same value for all the rare earths ($2c^*/7$, with $c^*=2\pi/c$).[2]

It has been shown that the application of chemical pressure reduces the CDW ordering temperature from values above 450 K for (La, Ce, Nd, and Pr)Te_3 to 244 K for $TmTe_3$.[8–10] Moreover, a reduction with chemical pressure of the single particle excitation frequency characteristic of the CDW state is accompanied by a decrease in the fraction of the Fermi surface that remains gapped, driving the samples toward a state of enhanced metallicity. This behavior was also observed in $CeTe_3$ with the application of external pressure,[11,12] extending the study of the above-mentioned phenomenon to even smaller lattice parameters than attainable through chemical pressure.

A second CDW ordering temperature has recently been discovered for the compounds with smaller lattice parameters (Tm, Er, Ho, and Dy).[9] In this case, the CDW is characterized by a wave-vector transverse to the first one and of larger value ($a^*/3$). This phase occurs at lower temperatures, dropping below 50 K for $DyTe_3$, and it increases with the application of chemical pressure. The shift of our attention to the CDW formation at low temperatures allows us to consider the effects caused on this state by other competing types of order. Cerium-based compounds frequently display an enhancement of their electronic effective mass at low temperatures caused by the strong hybridization of the localized $4f$ and conduction electron states and produce a variety of ground states, such as localized moment magnetic order[13] and superconductivity,[14] with many of these phases induced at high pressures.[15] The competing interaction of the CDW with some of these strongly correlated electron states by tuning chemical composition, pressure, or magnetic field is of particular interest in these materials.[16] In this paper, we present high-pressure electrical transport measurements on $CeTe_3$, along with the results of a subkelvin specific-heat experiment at ambient pressure and high magnetic fields. We have found that two magnetic phases occur below 20 K, with nonparallel magnetic easy axes, as can be inferred from the additional transport measurements made in fields for different angles. A possible structural phase transition suggested by features in the electrical resistivity at room temperature and at a pressure of 45 kbar, along with the low-temperature features detected at high pressures, may indicate the reduction in the CDW transition temperature below 300 K for the range of pressures used in our experiments.

II. EXPERIMENTAL DETAILS

Single crystals of $CeTe_3$ were grown by slow cooling of a binary melt as described elsewhere.[17] Electrical resistivity measurements under pressure were performed throughout the

temperature range 1.1 K$\leq T \leq$300 K, employing two different techniques. In the first technique, pressure was applied with a beryllium-copper piston-cylinder clamped cell using a Teflon capsule filled with a 1:1 mixture of *n*-pentane:isoamyl alcohol as the pressure transmitting medium to ensure hydrostatic conditions during pressurization at room temperature. The pressure in the sample chamber was inferred from the inductively determined pressure-dependent superconducting critical temperature of a lead manometer[18] and reached a maximum value of 23 kbar. In the second technique, pressure was applied in a beryllium-copper Bridgman-anvil clamped cell using solid steatite as the quasihydrostatic pressure transmitting medium. The pressure was determined from the superconducting transition of a strip of lead foil placed adjacent to the sample and measured using a four-lead resistive method. With this technique, a maximum pressure of 152 kbar was attained in the first attempt and 124 kbar in the second run. Pressure gradients were inferred from the width of the lead superconducting transition. These gradients were as large as 2% and 10% of the total pressure for the piston-cylinder and the Bridgman-anvil cell experiments, respectively. In both cases, the electrical resistance in the *ac* plane was measured using a four-lead technique and a Linear Research Inc. LR-700 ac resistance bridge. Resistivity measurements at ambient pressure were obtained using a quantum design physical property measurement system (PPMS) throughout the temperature range 1.9 K$\leq T \leq$20 K and for magnetic fields ranging from 0 to 9 T, applied both parallel and perpendicular to the *b* axis of the crystals.

The specific heat *C* of two single crystals with total mass of 7.5 mg was measured as a function of temperature *T* from 0.65 to 200 K using a ^{3}He semiadiabatic calorimeter and a standard heat-pulse technique for magnetic fields up to 5 T applied along the *b* axis.

III. RESULTS AND DISCUSSION

Electrical resistivity measurements as a function of temperature for different values of applied pressure are plotted in Fig. 1. The upper panel shows data obtained from the hydrostatic cell experiment for pressures up to 23 kbar, while the lower panel displays data taken in the Bridgman-cell experiments described in Sec. II and for pressures up to 152 kbar. At low pressures (hydrostatic cell, upper panel), the sample behaves as previously reported by Ru and Fisher,[17] although no appreciable local minimum at 10 K has been seen for these initial values of pressure. In our measurements, the resistivity decreases monotonically throughout the entire temperature range, which is more evident for the highest pressures obtained in the Bridgman-anvil cell (lower panel). Below 100 K, a broad hump denoted as T_ρ^*, which is clearly noticeable for the higher pressures, moves to lower temperatures to a value of 55 K at 50 kbar, after which it remains mostly unchanged for the higher pressures. This feature occurring at T_ρ^* is suggestive of the appearance of the charge-density wave order, which is supported by recent x-ray diffraction data obtained for $CeTe_3$ under pressure,[19] where it is clearly seen that the onset of the CDW state occurs below room temperature at 30 kbar. Nevertheless, the effects of the

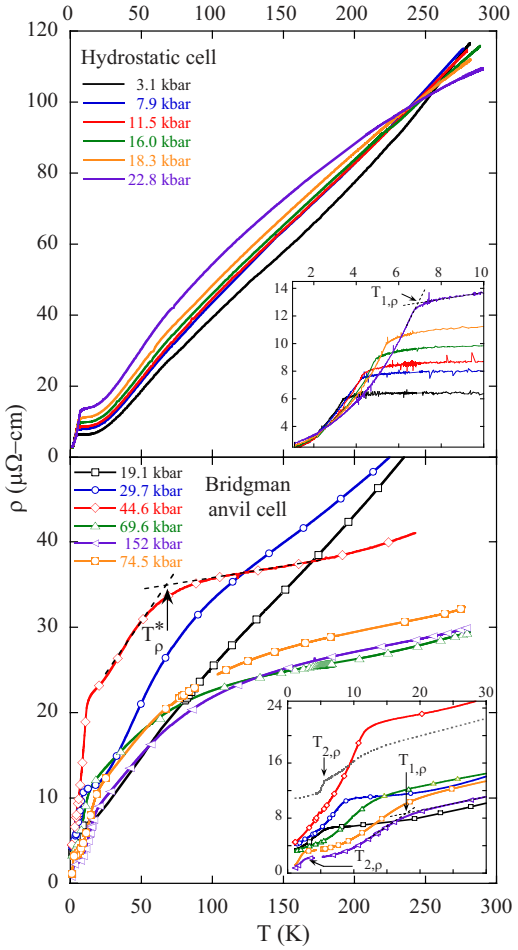

FIG. 1. (Color online) Electrical resistivity versus temperature at various pressures for $CeTe_3$ single crystals. Upper panel: hydrostatic cell experimental results. The inset shows the low-range, displaying the onset of the magnetic order as $T_{1,\rho}$. Lower panel: Bridgman-anvil cell results. The inset shows $T_{1,\rho}$, along with the new ordering temperature $T_{2,\rho}$, indicated in the figure for the first Bridgman run (for the 152 kbar curve) and for the second Bridgman run (in black, dashed curve).

crystalline electric field or the onset of Kondo coherence should not be ruled out, taking into account the strong hybridization of the localized 4*f* orbitals with the conduction band that usually takes place in cerium-based compounds. A lower temperature feature, labeled as $T_{1,\rho}$ was first reported by Iyeiri *et al.*[20] and later in the above-mentioned work by Ru and Fisher.[17] They attributed this feature to a transition to an antiferromagnetic state given the negative Curie-Weiss temperatures obtained from magnetic-susceptibility measurements. We found that this ordering temperature increases from 3 to 13 K under pressure, as can be seen in the insets of the upper and lower panels of Fig. 1. No appreciable change in $T_{1,\rho}$ is observed for pressures above 50 kbar. For pressures below 23 kbar, power-law fits to the resistivity curves below $T_{1,\rho}$ yielded exponent values averaging 2.2 ± 0.1.

A feature, occurring at a temperature denoted $T_{2,\rho}$, was discovered above 70 kbar for the two crystals measured in the two Bridgman experiments (lower inset of Fig. 1). The features are truncated at the base temperature of 1.1 K, where

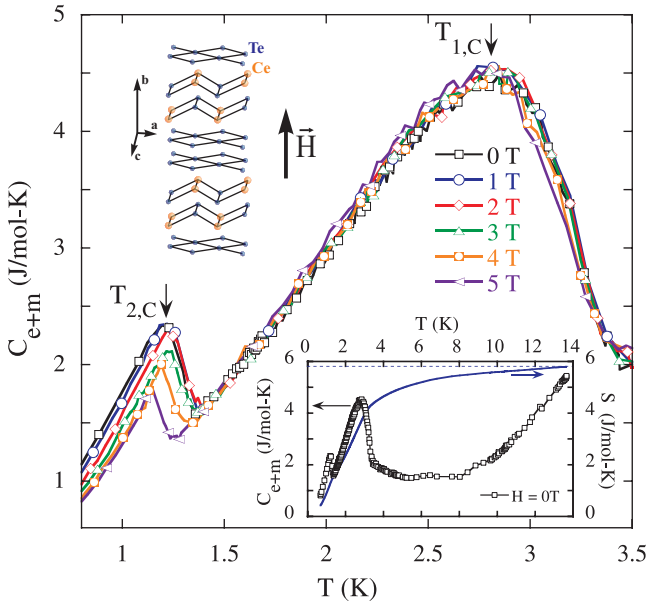

FIG. 2. (Color online) Electronic and magnetic contribution to the specific heat for different magnetic fields applied along the b axis of the $CeTe_3$ crystals. $T_{1,C}$ corresponds to the field-independent ordering temperature centered near 3 K, while $T_{2,C}$ denotes the field-dependent feature below 1.5 K. In the lower inset, the solid curve (blue) corresponds to the electronic and magnetic entropy in zero magnetic field and the horizontal dashed line corresponds to the value $R \ln 2$ J/mol K. The upper inset shows a schematic diagram of the crystal structure of $CeTe_3$ and the direction of the applied magnetic field in the specific-heat experiment.

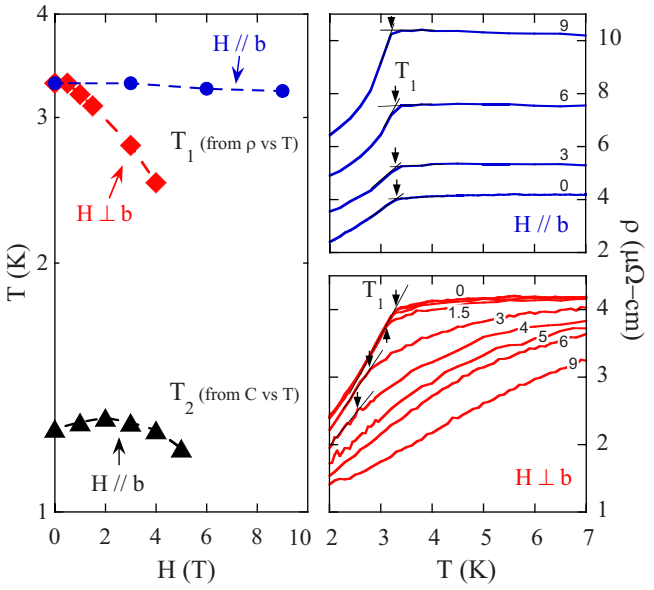

FIG. 3. (Color online) Left: field dependence of the magnetic ordering temperatures $T_{1,\rho}$ and $T_{2,C}$ of $CeTe_3$ for magnetic fields applied perpendicular and parallel to the b axis. A logarithmic temperature scale was chosen to emphasize the curvature of T_2 vs H. Right: temperature dependence of the electrical resistivity near T_1 for magnetic fields applied parallel (upper right: 0, 3, 6, and 9 T) and perpendicular (lower right: 0, 0.5, 1, 1.5, 3, 4, 5, 6, and 9 T) to the b axis of the crystals. The arrows mark the position of T_1. The numbers on each curve denote the value of the applied magnetic field in tesla. For the lower-right panel, arrows and numbers for fields of 0.5 and 1 T are not displayed for better clarity.

the resistivity has dropped by 65% of its value at the onset of the transition. In the first Bridgman-cell experiment, the drop of the resistivity was detected at 2.7 K and 152 kbar and it was seen again at 2.4 K and 74.5 kbar. For the second Bridgman run, $T_{2,\rho}$ remained at a value of 5.5 ± 0.1 K while increasing the pressure from 86 to 124 kbar. This suggests a possible new phase emerging at lower pressures and below the temperature range covered in this experiment. Figure 4 summarizes the different regions of the T-P phase diagram studied in the present work.

Figure 2 displays the electronic and magnetic contributions to the specific heat of $CeTe_3$ for magnetic fields up to 5 T applied along the b axis of the crystals obtained after subtracting the phonon contribution estimated from the high-temperature $C(T)$ data. The C/T versus T^2 fits yielded a Debye temperature of 161 K, comparable to previous values for $LaTe_3$, and an electronic specific-heat coefficient γ of 52 mJ/mol K^2, substantially larger than is observed for $LaTe_3$,[17] implying a moderately enhanced admixture of the localized $4f$ electron states of Ce with conduction electron states, as suggested in previously reported angle-resolved photoemission spectroscopy (ARPES) experiments.[4,6] A broad feature in $C(T)$ characterizing the magnetic order that occurs at $T_{1,C}$ corresponds directly to the transition temperature $T_{1,\rho}$ obtained from electrical resistivity measurements at ambient pressure (~3 K). This anomaly in the specific heat remains unchanged by the magnetic fields used in this experiment. The lower inset in Fig. 2 shows the electronic and magnetic contributions to the entropy at zero magnetic field, which adds up to $R \ln 2$ (indicated by a horizontal dashed line) at temperatures right above $T_{1,C}$, consistent with what is expected for a Ce^{3+}-doublet ground state.

At even lower temperatures, a sharper feature is observed in the $C(T)$ data that exhibits a rather weak-field dependence. This transition was not detected in the electrical resistivity experiments (down to 1.1 K). This suggests that this new phase also has a magnetic origin. The transition temperature $T_{2,C}$ (defined after performing an equal-entropy analysis of the data) increases to a value of ~1.3 K at 2 T and then decreases for the higher applied fields. The left panel of Fig. 3 illustrates the evolution of this feature throughout the range of applied magnetic fields in which the specific-heat measurements were made.

The above evidence associated with the low-temperature transition below 1.5 K and the apparent lack of field dependence for the 3 K ordering temperature revealed by the specific-heat data led us to inquire further into the origin of these magnetic transitions. The work by Iyeiri *et al.*,[20] previously mentioned, foretells a strong dependence of the magnetic phases of $CeTe_3$ with the orientation of the applied magnetic field with respect to the crystalline axes. In order to test the angle dependence of T_1, electrical resistivity measurements were performed down to 2 K in magnetic fields ≤ 9 T applied perpendicular and parallel to the b axis of the crystals and perpendicular to the direction of the current passing through the ac planes of the samples, utilizing a

commercial quantum design PPMS sample rotator. The two right panels of Fig. 3 show these results. With magnetic fields applied perpendicular to the planes ($H \| b$, upper-right panel), the transition temperature T_1 does not shift with applied magnetic field, consistent with the specific-heat measurements, although a rather strong magnetoresistance was found $[(R_{9T}-R_0)/R_0=1.43$ at 10 K]. On the other hand, for fields applied parallel to the *ac* planes (lower-right panel), a negative magnetoresistance is observed, and the transition temperature T_1 moves toward zero as indicated by the arrows. The left panel in Fig. 3 combines the field dependencies of $T_{1,\rho}$ for $H \| b$ and $H \perp b$, with the field dependence of $T_{2,C}$ with $H \| b$.

Although not shown in Fig. 3 for clarity, the local Kondo-type minimum around 10 K mentioned earlier[4,17] has been seen in this set of measurements at ambient pressure. For $H \| b$, this minimum appears at 9.8 K without applied magnetic field and increases to 10.5, 12, and 13 K for 3, 6, and 9 T. For $H \perp b$, the minimum observed at zero field at 9.8 K remains unchanged for fields below 1.5 T and then disappears for magnetic fields above 3 T.

The specific-heat and transport data presented in Figs. 2 and 3 suggest that T_1 characterizes the onset of the transition to a magnetic phase with the easy magnetic axis contained in the *ac* planes. The *b* axis would then play the role of a hard axis for this magnetic phase, consistent with magnetic-susceptibility measurements.[20] In the case of the transition at $T_{2,C}$, we did not measure the specific heat with the magnetic field applied parallel to the basal plane, but we can conclude that the $T_{2,C}$ magnetic easy axis is not parallel to the T_1 easy axis, as can be found in other anisotropic magnetic *f*-electron systems reported elsewhere,[21] in which ferromagnetic and antiferromagnetic phases occur at different ordering temperatures, with noncollinear ordering directions, due to the interaction of the localized *f* electrons with the conduction electrons (intra-atomic exchange) and with nearby ions (interatomic exchange) and to the effect of crystalline electric fields.

The temperature vs pressure phase diagram is presented in Fig. 4. It is clearly seen that the curve $T_1(P)$ saturates to a rather constant value above 50 kbar. $T^*(P)$ also shows a kink around the same pressure and then attains a constant value of ~55 K. This particular value of pressure separates the phase diagram in two regions: a low-pressure region where the phase characterized by $T^*(P)$ competes with the phases below $T_1(P)$ and a high-pressure region where these three phases may coexist. The inset of Fig. 4 shows the room-temperature dependence of the electrical resistance with applied pressure (compression only). An abrupt drop of the resistance occurs around 45 kbar, suggesting the existence of a structural phase transition at this pressure. Despite the fact that this feature in the electrical resistance was observed at room temperature, the value of this pressure coincides with the kinks in the $T^*(P)$ and $T_1(P)$ curves at 50 kbar, and with the emergence of the critical temperature $T_{2,\rho}$ above 60 kbar. As we previously mentioned, in a recent work by Sacchetti *et al.*,[19] x-ray diffraction experiments performed under pressure showed that the satellite peaks associated with the CDW lattice distortion disappear at room temperature when an external pressure of 30 kbar is applied. This suggests that the

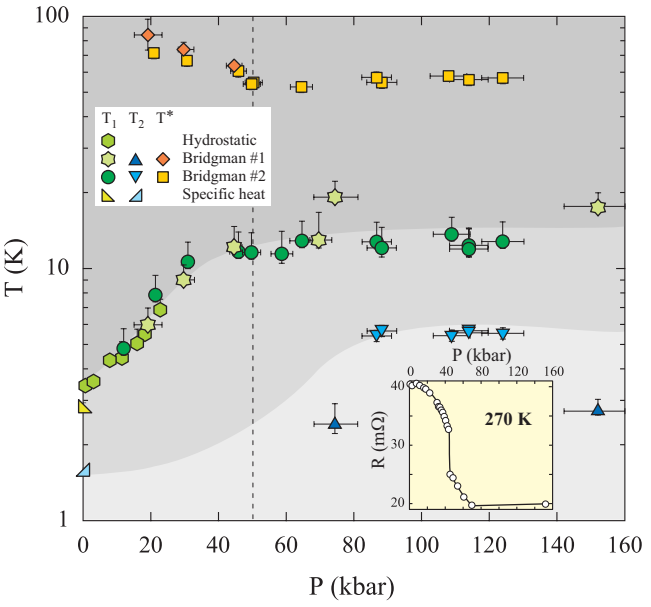

FIG. 4. (Color online) Temperature versus pressure phase diagram for $CeTe_3$ (note the logarithmic temperature scale). T^* characteristic temperature associated with the "humplike" feature in $\rho(T)$, possible origins of which are discussed in the text; T_1 magnetic ordering temperature; T_2 ordering temperature (probably magnetic). The vertical dashed line separates the *T*-*P* phase diagram into two regions in which T^*, T_1, and T_2 all have distinctly different pressure dependencies. We grouped in a single low-temperature magnetic phase the critical temperatures T_2 obtained from measurements of the electrical resistivity under pressure and specific heat at ambient pressure, although they might have different origins. Inset: room-temperature evolution of the electrical resistance as the pressure was increased. The abrupt jump at 45 kbar may be due to a structural phase transition.

onset of the CDW transition is driven to lower temperatures when high enough pressures are applied to the rare-earth tritellurides. In the same report, the authors showed that the *a* and *c* lattice parameters become equal at room temperature and for pressures above 30 kbar, which is indicative that a structural phase transition might be taking place near that value of pressure. Unfortunately, no x-ray data under pressure and at low temperatures has yet been reported for $CeTe_3$, which would definitely clarify the origin of T^* that we found in our Bridgman-cell experiments.

IV. CONCLUSIONS

In summary, we have presented high-pressure, transport, and thermodynamic measurements on $CeTe_3$ single crystals. These measurements yielded evidence for two magnetic phases detected in electrical resistivity and specific-heat measurements at low temperatures, with nonparallel magnetic easy axes. We also reported the emergence of a phase at high pressures and low temperatures and a possible structural transition detected at room temperature and at 45 kbar, which could be related to the reduction in the CDW transition temperature, illustrating that external pressure plays a key role in establishing the phase diagram of the highly anisotropic rare-earth tritellurides.

ACKNOWLEDGMENTS

Research at University of California, San Diego was supported by the National Nuclear Security Administration under the Stewardship Science Academic Alliance Program through the U. S. Department of Energy (Grant No. DE-FG52-06NA26205). Crystal growth at Stanford University was supported by the U. S. Department of Energy (Contract No. DE-AC02-76SF00515).

[1] G. Grüner, *Density Waves in Solids* (Addison-Wesley, Reading, MA, 1994).
[2] E. DiMasi, M. C. Aronson, J. F. Mansfield, B. Foran, and S. Lee, Phys. Rev. B **52**, 14516 (1995).
[3] V. Brouet, W. L. Yang, X. J. Zhou, Z. Hussain, N. Ru, K. Y. Shin, I. R. Fisher, and Z. X. Shen, Phys. Rev. Lett. **93**, 126405 (2004).
[4] V. Brouet, W. L. Yang, X. J. Zhou, Z. Hussain, R. G. Moore, R. He, D. H. Lu, Z. X. Shen, J. Laverock, S. B. Dugdale, N. Ru, and I. R. Fisher, Phys. Rev. B **77**, 235104 (2008).
[5] B. K. Norling and H. Steinfink, Inorg. Chem. **5**, 1488 (1966).
[6] H. Komoda, T. Sato, S. Souma, T. Takahashi, Y. Ito, and K. Suzuki, Phys. Rev. B **70**, 195101 (2004).
[7] P. Villars, *Pearson's Handbook Desk Edition: Crystallographic Data for Intermetallic Phases* (ASM International, Materials Park, OH, 1997), Vol. 1, p. 1221.
[8] A. Sacchetti, L. Degiorgi, T. Giamarchi, N. Ru, and I. R. Fisher, Phys. Rev. B **74**, 125115 (2006).
[9] N. Ru, C. L. Condron, G. Y. Margulis, K. Y. Shin, J. Laverock, S. B. Dugdale, M. F. Toney, and I. R. Fisher, Phys. Rev. B **77**, 035114 (2008).
[10] N. Ru, J.-H. Chu, and I. R. Fisher, Phys. Rev. B **78**, 012410 (2008).
[11] A. Sacchetti, E. Arcangeletti, A. Perucchi, L. Baldassarre, P. Postorino, S. Lupi, N. Ru, I. R. Fisher, and L. Degiorgi, Phys. Rev. Lett. **98**, 026401 (2007).
[12] M. Lavagnini, A. Sacchetti, C. Marini, M. Valentini, R. Sopracase, A. Perucchi, P. Postorino, S. Lupi, J. H. Chu, I. R. Fisher, and L. Degiorgi, Phys. Rev. B **79**, 075117 (2009).
[13] S. Süllow, M. C. Aronson, B. D. Rainford, and P. Haen, Phys. Rev. Lett. **82**, 2963 (1999).
[14] M. H. Jung, A. Alsmadi, H. C. Kim, Yunkyu Bang, K. H. Ahn, K. Umeo, A. H. Lacerda, H. Nakotte, H. C. Ri, and T. Takabatake, Phys. Rev. B **67**, 212504 (2003).
[15] N. D. Mathur, F. M. Grosche, S. R. Julian, I. R. Walker, D. M. Freye, R. K. W. Haselwimmer, and G. G. Lonzarich, Nature (London) **394**, 39 (1998).
[16] C. Berthier, P. Molinié, and D. Gérome, Solid State Commun. **18**, 1393 (1976).
[17] N. Ru and I. R. Fisher, Phys. Rev. B **73**, 033101 (2006).
[18] B. Bireckoven and J. Wittig, J. Phys. E **21**, 841 (1988).
[19] A. Sacchetti, C. L. Condron, S. N. Gvasaliya, F. Pfuner, M. Lavagnini, M. Baldini, M. F. Toney, M. Merlini, M. Hanfland, J. Mesot, J.-H. Chu, I. R. Fisher, P. Postorino, and L. Degiorgi, arXiv:0811.0338v1 (unpublished).
[20] Y. Iyeiri, T. Okumura, C. Michioka, and K. Suzuki, Phys. Rev. B **67**, 144417 (2003).
[21] R. J. Elliott, Phys. Rev. **124**, 346 (1961).